Reactions in nanofilms of trifluoroacetic acid (CF₃COOH) driven by low energy electrons

Mario Orzol [a], Tibor Sedlacko [a], Richard Balog [a,1], Judith Langer [a,*], Grzegorz P. Karwasz [a,2],
Eugen Illenberger [a], Anne Lafosse [b], Mathieu Bertin [b], Alicja Domaracka [b,3], Roger Azria [b]

[a] *Institut für Chemie und Biochemie, Physikalische und Theoretische Chemie Freie Universität Berlin, Takustrasse 3, D-14195 Berlin, Germany*
[b] *Laboratoire des Collisions Atomiques et Moléculaires, CNRS-Université Paris-Sud (UMR 8625, FR LUMAT) Bât. 351,*
Université Paris-Sud, F-91405, Orsay Cedex, France

Abstract

Electron stimulated desorption (ESD) of fragment anions and thermal desorption spectroscopy (TDS) is applied to study reactions in thin films of a few CF₃COOH/CF₃COOD monolayers following low energy electron impact (0–20 eV). In ESD, the fragment ions H^-/D^- and F^- are observed via resonant features in the energy range 5–12 eV similar to the dissociative electron attachment (DEA) resonances present in gas phase CF₃COOH. Extended electron irradiation of the film at energies above 9 eV generates CO_2 and CHF_3/CF_4 as revealed by a combination of TDS and ESD experiments. The yield for these reactions continuously increases with energy indicating that they are initiated via electronically excited neutrals rather than negative ion resonances. No reactions induced by sub-excitation electrons (≈ 1 eV) could be observed using the present experimental techniques. In a very recent study on electron attachment to clusters of CF₃COOH [J. Langer, I. Martin, G. Karwasz, E. Illenberger, Int. J. Mass Spectrom. Ion Processes 249/250 (2006), 477], the ion–molecule complex $CF_3COO^- \cdot H_2O$ appeared as strongest signal via a resonance located at 0.4 eV.

1. Introduction

We study electron driven reactions in thin films of perfluoroacetic acid (CF₃COOH) by means of electron stimulated desorption of fragment anions (ESD) and thermal desorption spectroscopy (TDS), the latter following irradiation of the film at defined electron energies in the range 0–20 eV. The present work is the outcome of a collaborative study between the Berlin laboratory and the Orsay laboratory in the framework of the EU Network EPIC (Electron and Positron Induced Chemistry). It follows previous experiments on electron driven reactions in sin-

gle gas phase molecules (under single collision conditions) [1] and in gas phase clusters generated by supersonic beam expansion [2]. CF₃COOH is frequently used in organic synthesis as solvent [3] and also as catalyst for polymerization reactions [4]. It can be detected in trace amounts around the globe in soils, plants and waters. It is believed that it is formed from the decomposition of halocarbons [5].

In the previous gas phase experiments [1] two resonant features were observed located near 1 eV and around 8 eV, assigned as shape resonance and core excited resonance, respectively. The dominant decomposition products of the shape resonance are identified as CF_3COO^- and CF_2COO^- arising from the dissociative electron attachment (DEA) reactions:

$$e^- + CF_3COOH \rightarrow CF_3COO^- + H \tag{1}$$

$$e^- + CF_3COOH \rightarrow CF_2COO^- + HF \tag{2}$$

associated with the loss of an H atom and an HF molecule, respectively. The core excited resonance additionally decomposes into F^-, CF_3^- and CO_2^-. The latter ion is considered

metastable having a sufficiently long lifetime for mass spectrometric detection [6].

Electron attachment to clusters of trifluoroacetic acid revealed interesting features as (a) the cross section for negative ion formation at low energies (0–1 eV) significantly increases and (b) in addition to the ions known from DEA to single CF_3COOH molecules a variety of larger complexes is observed. The underlying reactions are assigned as intracluster DEA leading to solvated fragment ions, and (evaporative) *associative electron attachment* resulting in non-decomposed cluster ions including the monomer. The most intense signal, however, is due to the ion–molecule complex $CF_3COO^- \cdot H_2O$ which is the result of a chemical reaction initiated by the attachment of electrons at an energy of 0.4 eV to the neutral hydrogen bonded dimer.

The goal of the present investigation is to study the response of the CF_3COOH system towards low energy electrons when going to the condensed phase. It is well established that negative ion resonances are often preserved when proceeding from the gas phase to the corresponding molecular films [7,8]. Such resonances can directly be observed by mass spectrometric techniques under conditions when the ionic DEA product is ejected into vacuum (electron stimulated desorption). Extended electron irradiation of the film can lead to a chemical transformation which can be followed by the evolution of the ESD signal during irradiation [9] but also by analysis of the irradiated film via thermal desorption spectroscopy [10].

It should be noted that the present CF_3COOH film cannot be viewed as an assembly of single molecules coupled by weak intermolecular forces (like in many films of small organic molecules [8]). From the tendency of the present acid to form O–H and F–H bridges we can rather expect that the film and its surface consist of a molecular network coupled by the comparatively stronger hydrogen bonds.

2. Experimental

The experiments were performed within a coordinated study at the Berlin and at the Orsay Laboratory. While at Orsay the ESD data on freshly deposited films of CF_3COOH/CF_3COOD were carried out, extended electron irradiation of the films and analysis via TDS was conducted in the Berlin laboratory. The Berlin ultra high vacuum (UHV) apparatus consists of a trochoidal electron monochromator [11], a cryogenically cooled Au (1 1 1) mono-crystalline substrate mounted on a manipulator and a commercial quadrupole mass spectrometer (QMS) with an ion extraction system as described earlier [8]. The substrate can be cooled down to approximately 40 K (as measured by a thermocouple mounted directly on the crystal) by means of a closed-cycle He refrigerator and heated resistively up to 800 K.

The electron monochromator uses a weak homogeneous magnetic field (15 G) which prevents the spreading of the electron beam. The background pressure is in the 10^{-10} mbar range, rising after a longer series of measurements to 2×10^{-9} mbar. The energy resolution is about 0.3 eV as derived from the steepness of the onset of the electron injection curve into the uncovered substrate. The electron energy scale refers to vacuum zero

and is also calibrated by the onset of the injection curve. Film charging in the course of electron irradiation results in a shift of the onset of the injection curve with respect to the monochromator potential. Since the onset is taken as reference, charging of the film will not affect the energy scale.

The Orsay apparatus [12] consists of an electron monochromator, an electrically insulated hydrogenated diamond substrate fixed on the cold end of a He-cryostat, a QMS in line with an energy selective filter (referred to as the energy mass analyser) to detect electrons or desorbing ions, and an additional independent fixed QMS. These different elements are housed in an UHV chamber (base pressure below 8×10^{-11} mbar) equipped with two μ-metal foils to reduce the magnetic field to below 5 mG. The electron source is a hemispherical monochromator. A computer controlled electrostatic zoom lens focuses the 1–10 nA electron beam onto the sample. The desorbed ions are either energy selected with a hemispherical analyser and separated from the electrons by means of the in line QMS or directly mass analyzed with the fixed QMS. The energy of the incident electron beam and of the desorbing ions were calibrated with respect to the vacuum level to within ± 0.2 eV by a measurement of the electron energy loss spectra of the substrate covered by the condensed trifluoroacetic acid. The electron gun and the energy mass analyzer are mounted on rotatable stages having the cryostat on axis, the other QMS is fixed normal to the substrate.

Trifluoroacetic acid (or its deuterated analogue CF_3COOD) is condensed by exposing the substrate to a volumetrically calibrated effusive outflow from a capillary located 7 mm from the crystal. For the evaluation of the film thickness we assume 100% sticking of the gas on the crystal. Typically three monolayers (ML) were used.

Electron stimulated desorption is performed by recording the negative ion yield at a defined mass as a function of the energy from a freshly deposited film. Successive scans can change the shape and intensity of the signal and contain information on reactions due to electron irradiation. In addition to ESD, samples of CF_3COOH and CF_3COOD are irradiated at a fixed electron energy and dose and then studied by thermal desorption spectroscopy. The evaporated material is ionized by 70 eV electrons and analyzed by the quadrupole mass spectrometer. Since the ionization process is generally associated with fragmentation of the parent cation the mass spectrum alone is generally ambiguous. Observation of mass 44 (CO_2^+) can arise from fragmentation of CF_3COOH molecules following electron impact ionisation:

$$e^- + CF_3COOH \rightarrow 2e^- + CF_3COOH^{+\#} \rightarrow CO_2^+ + \cdots \quad (3)$$

or as a result from ionization of neutral CO_2 previously formed by a chemical reaction in the film during electron irradiation. These two cases, however, can easily be distinguished by their different evaporation temperature. In the present measurements the temperature rise was about 0.7 K s^{-1}. The accuracy of the temperature scale was accurate within about 10 K.

We also use the deuterated analogue CF_3COOD to discriminate against possible reactions from some background H_2O. The observation is that in the inlet system CF_3COOD is effectively

transferred into CF$_3$COOH due to D/H exchange during collision with the walls covered by the previously used CF$_3$COOH and other hydrogen containing molecules. To minimize this effect the inlet system has to be heated and several fill and pump cycles using CF$_3$COOD have to be applied. By this means, the degree of deuteration in the condensed sample can be increased to more than 50%. CF$_3$COOH and CF$_3$COOD were purchased from Fluka and Sigma–Aldrich (stated purity 99 and 99.5%, respectively) and used as delivered.

3. Results and discussion

In order to extract information on electron driven reactions in the CF$_3$COOH film we use electron stimulated desorption of fragment ions and thermal desorption spectroscopy. ESD at a freshly deposited film gives direct access to the *primary* reaction induced by electron impact. If a molecule is subjected to DEA at or near the surface, the associated fragment ion may be observed by a mass spectrometer as desorbed ion under particular kinematic and structural prerequisites (see below). On the other hand, extended irradiation of the molecular film (either via successive ESD scans or irradiation at a particular electron energy) can lead to a chemical transformation of the film, which will generally affect the ion yield in ESD (intensity and shape). In a few special cases, the transformation of a molecular film following electron irradiation can completely be monitored via ESD. By this method, we have recently followed the transformation of C$_2$F$_4$Cl$_2$ into Cl$_2$ (plus perfluorinated by-products) [9]. By irradiating the film sufficiently long with electrons at sub-excitation energies, such a transformation can be made complete [13]. In TDS we analyse the desorbing *neutral* material as a function of the temperature of desorption by positive mass spectrometry. TDS is usually applied after extended irradiation of the sample at a defined electron energy and dose.

3.1. Electron stimulated desorption (ESD) of fragment Ions

The interaction of a freshly deposited CF$_3$COOD film (3 ML) with low energy electrons leads to desorption of F$^-$ and D$^-$, see Fig. 1c and d. Both signals show a resonant structure indicating that DEA at or near the surface is the underlying reaction. For comparison, Fig. 1 also presents the two prominent ionic products arising from DEA to single CF$_3$COOH molecules, namely CF$_3$COO$^-$ (Fig. 1a) originating from hydrogen loss (1) via the low energy shape resonance near 1 eV and F$^-$ (Fig. 1b) which is mainly formed through a broader resonant like feature in the energy range between about 5 and 12 eV. The structure of the ion yield at higher energies (gas phase and condensed phase) indicates that different energetically overlapping resonances contribute to the overall ion yield. It remains under question whether the corresponding precursor states are core excited resonances or shape resonances. We mention here that quantum scattering calculations [14] carried out on the formic acid dimer in fact predict shape resonances also at higher energies. Irrespective of the detailed classification of these electronic states, the comparison indicates that the resonances at higher
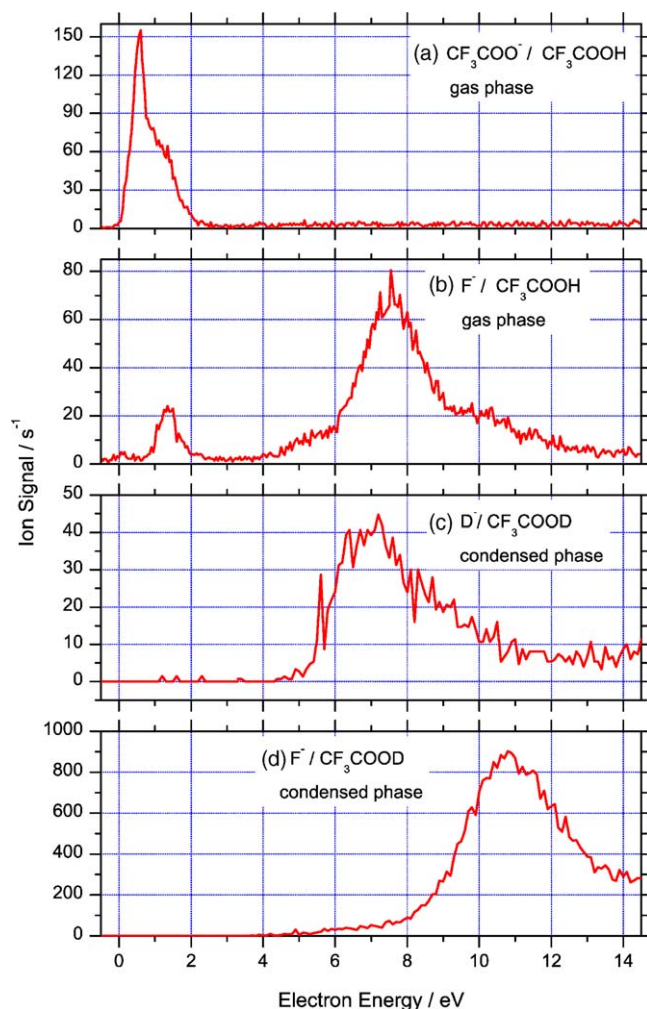

Fig. 1. Comparison between two abundant fragment ions (a) CF$_3$COO$^-$ and (b) F$^-$ obtained from dissociative electron attachment (DEA) to gas phase CF$_3$COOH and the two fragment ions (c) D$^-$ and (d) F$^-$ observed from electron stimulated desorption from a 3 ML CF$_3$COOD film.

energies are preserved in the condensed phase as obvious by comparing the F$^-$ signal from both phases. They appear, however, at different relative intensities. The F$^-$ desorption signal is relatively enhanced on the higher energy part of the core excited feature. The origin of this behaviour is not directly obvious as the relative intensity of the signal is nearly independent from the orientation of the sample with respect to the electron beam and the quadrupole axis. Also the analysis of the kinetic energy distributions of F$^-$ revealed that they do not noticeably change with the incident electron energy. The most probable energy is at 0.8 eV and hence the difference between the shape of the ion yield between gas phase DEA and ESD is not due to particular kinetic energy release effects.

We have no information on H$^-$ formation from the gas phase molecule since the mass spectrometer used in the gas phase experiment [1] was not capable to analyse H$^-$. In recent DEA experiments on formic acid (HCOOH) [15] and acetic acid (CH$_3$COOH) [16] performed at the Innsbruck laboratory, no H$^-$ formation could be detected while in experiments with much higher sensitivity (non-monochromatized electron beam)

H^- was readily observed from acetic acid within a series of three overlapping resonances peaking at 6.7, 7.7, and 9.1 eV [17].

As mentioned above, CF_3COOH has the tendency to form hydrogen bridges with the dimer as a particular stable configuration. Under the conditions of an effusive beam, the data indicate that only monomers of CF_3COOH are present [1] (which is also consistent with a thermodynamic treatment of the system under the correspondingly low pressure). In the supersonic beam, the dimer is the predominant species [2] although larger complexes (possibly associated via F–H bridges) are present. We can hence expect that the condensed film also consists of a network of CF_3COOH molecules coupled by hydrogen bonding. Under such conditions the resonances at higher energies are obviously preserved as Figs. 1c and 1d show.

The two prominent ions observed in gas phase DEA (CF_3COO^-, CF_2COO^-) are not detected as desorption products as expected from the energetic and kinematic requirements for desorption. Apart from the orientation of the molecule at the surface, a fragment ion can only escape into vacuum if its kinetic energy exceeds its polarization energy with the environment, i.e., the fragment ion must gain sufficient kinetic energy from the decomposition process. For a molecular film consisting of molecules which are coupled through weak intermolecular forces one can describe the reaction as resonant electron capture of an individual molecule at the surface following unimolecular decomposition of the transient negative ion (TNI) finally leading to desorption of the ionic fragment. Taking into account that both the TNI and the fragment ion are subjected to the (same) polarization energy V_a, and applying the principle for conservation of energy and momentum one obtains a simple relation expressing the threshold energy for desorption E_d as [18]:

$$E_d = (m_i/m)V_a + \Delta H_0 \tag{4}$$

with m_i and m are the mass of the ionic and neutral fragment, respectively, and ΔH_0 is the thermodynamic threshold of the corresponding gas phase DEA process. Note that in this context V_a is a positive number with ≈ 1 eV a reasonable number for many organic molecules [19]. Irrespective of the detailed structure of the compound at the surface, expression (4) indicates that desorption of light ions is in any case preferred. The fact that the D^- desorption signal is even lower than that of F^- then in fact indicates that the cross section for the *intrinsic* DEA reaction D^-/CF_3COOD is extremely weak.

The gas phase F^- spectrum shows a signal in the range of the low energy shape resonance (1.5 eV), appreciably weaker than that at higher energy (7.5 eV). On first sight, such a behaviour for a gas phase DEA signal appears surprising since the general tendency of the electron attachment cross section is to increase towards low energies [20]. In fact, a closer look on the energetics and also the underlying mechanism of the reaction provides a reasonable explanation: The thermodynamic threshold for F^- is dictated by the relation $\Delta H_0 = D(C - F) - EA(F)$, with D the bond dissociation energy and EA the electron affinity. By taking $D(C - F) \approx 5$ eV and $EA(F) = 3.4$ eV (Table 1 [21]) we arrive at $\Delta H_0 = 1.6$ eV. Hence, the DEA channel yielding F^-

Table 1
Gas phase heats of formation (ΔH_f°) and electron affinities (EA) for compounds relevant in the present reactions, taken from Ref. [21]

Compound	ΔH_f° (kJ mol^{-1})
CF_3COOH	−1031.4
CHF_3	−697
CF_4	−930
C_2F_6	−1344
H_2O	−241.8
CO_2	−393.5
CF_2H_2	−450.6
CO	−110.5

Compound	EA (eV)
F	3.4
H	0.75

is energetically only accessible within the high energy tale of the low energy shape resonance. In addition, this resonance has π^* character with the excess electron initially localized on the COO site. F^- formation then proceeds through intra-molecular charge and energy transfer (vibrational predissociation) which explains its low intensity in the gas phase. Accordingly, such a rather indirect dissociation mechanism hardly provides sufficient kinetic energy for the F^- ion to escape from the surface.

As already mentioned above, the maximum of the F^- desorption yield peaks at higher energy compared to the prominent peak in the gas phase DEA spectrum. This effect is not due to a particular orientation of the surface or the appearance of a particular kinetic energy release. At this point we shall not discuss this problem in more detail but only state that the probability distribution in ESD (the ion yield) is principally the result of the initial Franck–Condon transition creating the transitory ion convoluted with the (energy dependent) probability for desorption. This can lead to a maximum in the ESD yield which is shifted to either higher or lower energies with respect to that of the gas phase DEA yield, dependent on which effect dominates. It should finally be noted that the coupling of an excited resonance to its environment is a complicated matter and does not necessarily result in the usual polarization shift to lower energies as this is the case for ground state ions. The overall ion yield above 5 eV most likely originates from different, energetically overlapping resonances with their electronic structure not yet assigned.

To summarise the ESD results it is evident that both D^- and F^- are formed via DEA involving resonances which are also present in gas phase CF_3COOH/CF_3COOD. No ESD signal in the energy range of the low energy shape resonance is observed. This does, however, not necessarily imply that in the condensed material low energy electron driven reactions are not operative. To track this problem, we have carried out extended irradiation experiments with subsequent analysis of the adsorbate by thermal desorption spectroscopy. In addition, further studies of low energy electron induced processes by means of high resolution electron energy loss spectroscopy (HREELS) are currently performed at the Orsay Laboratory.

3.2. Reactions induced by extended electron irradiation/thermal desorption spectroscopy (TDS)

Reactions in condensed material induced by low energy electrons (<20 eV) have been the subject of many investigations within the last years. Among these, we mention ozone synthesis in an oxygen film [22], CO formation in condensed acetone [23], Cl_2 formation from a $C_2F_4Cl_2$ film [9,13] or CO_2 formation in formic acid, HCOOH [10]. At least for ozone synthesis from O_2 and Cl_2 synthesis (from $C_2F_4Cl_2$) it was clear that the reaction is initiated by DEA. In $C_2F_4Cl_2$ a complete transformation of the film was obtained by using electrons at sub-excitation energies [13].

Fig. 2 shows two thermal desorption spectra after the CF_3COOH film (freshly deposited in both cases) has been irradiated by electrons at 9 and 15 eV, respectively (40 nA, 600 s). The spectra are recorded via the 44 amu signal (CO_2^+) which is a representative member of the fragmentation pattern in the mass spectrum of CF_3COOH at 70 eV electron impact [24]. Since the non-irradiated film only shows a feature around 160 K (not presented here) we ascribe the peak near 160 K in Figs. 2a and 2b
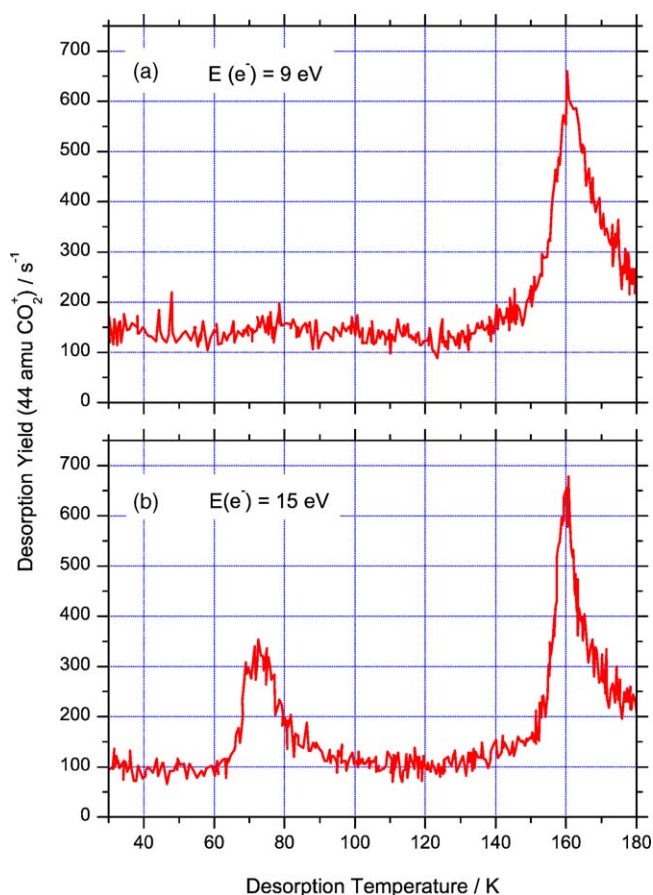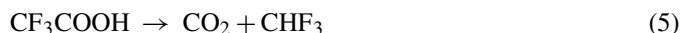

Fig. 2. Thermal desorption spectrum from CF_3COOH films recorded on the 44 amu ion (CO_2^+) following irradiation with electrons of (a) 9 eV and (b) 15 eV (film thickness: 3 ML; electron intensity: 40 nA; irradiation time: 600 s). The spectrum at 9 eV closely resembles that of a non-irradiated film and the feature near 160 K is due to desorption of CF_3COOH. The new feature appearing at low temperature after 15 eV irradiation is considered to arise from desorption of CO_2 formed under electron impact to the film (see the text).

to desorption of intact CF_3COOH molecules. After irradiation with electrons at energies above 9 eV a new structure gradually appears in the TDS corresponding to material already desorbing at distinctly lower temperatures (around 70 K, see Fig. 2b). This new feature can be ascribed to the desorption of CO_2 produced during irradiation: CO_2^+ is the dominant ion in the mass spectrum of gas phase CO_2 and the vapour pressure of condensed CO_2 increases from 10^{-11} at 65 K to 10^{-8} mbar at 76 K [25]. This corresponds to the experimental situation with the chamber background pressure at 10^{-10} mbar rising into the 10^{-8} mbar range during thermal desorption.

During irradiation the ratio in the intensity of the two desorption peaks (75/165 K) levels off already at an irradiation time of about 10 min corresponding to a dosage of 24 μC or about 10^{14} electrons impinging on an area of about 0.3 cm². This mirrors some equilibrium between CF_3COOH and CO_2, already established at that dosage. A search in the energy range around 1 eV, where the pronounced shape resonance is present (visible in DEA to single CF_3COOH molecules and clusters), did not show any signature of CO_2 formation. We note, however, that current HREELS experiments at Orsay in fact show CO_2 formation at an irradiation energy of 1 eV [26] indicating that the low energy resonance is involved in CO_2 formation and at higher irradiation dose that HREELS is more sensitive than the presently applied desorption technique.

The energetically lowest pathway for carbon dioxide formation from CF_3COOH is coupled with formation of trifluoromethane according to

$$CF_3COOH \rightarrow CO_2 + CHF_3 \qquad (5)$$

In the gas phase this reaction is exothermic by -59 kJ mol^{-1} (Table 1), but subject to an appreciable activation barrier.

To check whether also trifluoromethane is formed we performed thermal desorption spectroscopy by recording CF_3^+ (69 amu), the dominant ion in the mass spectrum of CHF_3 and the second intense in CF_3COOH, and also ESD on a pure CHF_3 film.

Fig. 3 shows a sequence of desorption spectra obtained at 69 amu. The non-irradiated film exhibits the usual desorption characteristics of CF_3COOH with a peak near 165 K. At 130 K a small satellite peak is visible, the origin of which is not clear. It may arise from molecules with lower adsorption energy (not coupled in the hydrogen bonded network). At an irradiation energy of about 3 eV this satellite peak appears at lower temperature (120 K) and one can speculate whether this signal is due to the homolytic C–C bond cleavage generating the neutral radicals CF_3 and COOH.

Near 10 eV, finally, a new CF_3^+ desorption feature appears at distinctly lower temperature ($\approx$60 K) indicating the generation of a more volatile compound. This signal may be attributed to desorption of CHF_3, which is supported by the observation that desorption of a pure CHF_3 film (not shown here) occurs at $\approx$60 K as observable on the CF_3^+ signal.

To obtain complementary information we have applied ESD on pure CHF_3. Fig. 4c shows the F$^-$ desorption signal from a freshly deposited CHF_3 film yielding a comparatively weak
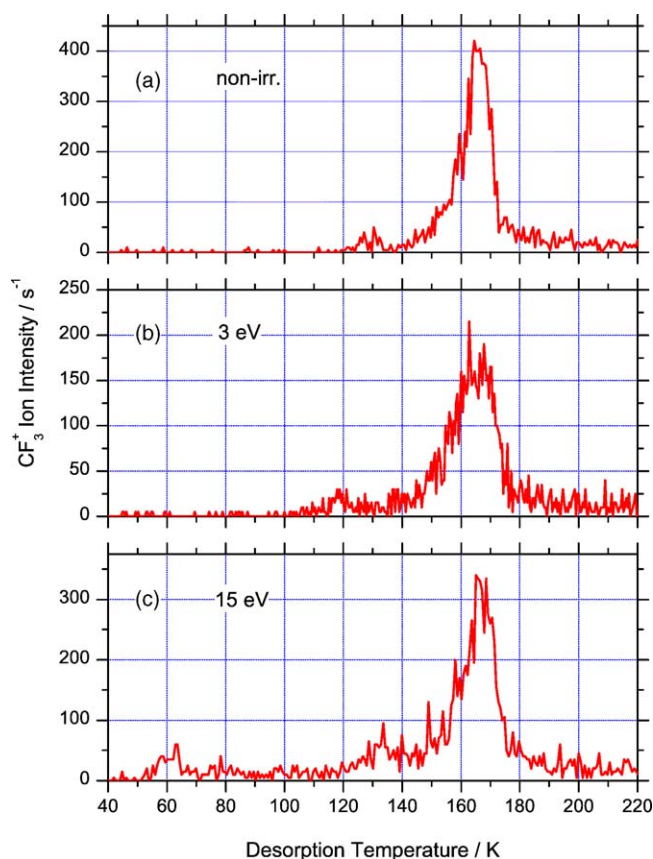
Fig. 3. Thermal desorption spectra from a 3 ML film of CF_3COOH obtained on the 69 amu signal (CF_3^+) after irradiation with different energies: (a) without irradiation, (b) with 3 eV and (c) with 15 eV. The feature appearing at low temperature after irradiation with 15 eV electrons is considered to arise from desorption of CHF_3 and/or CF_4 (see the text).
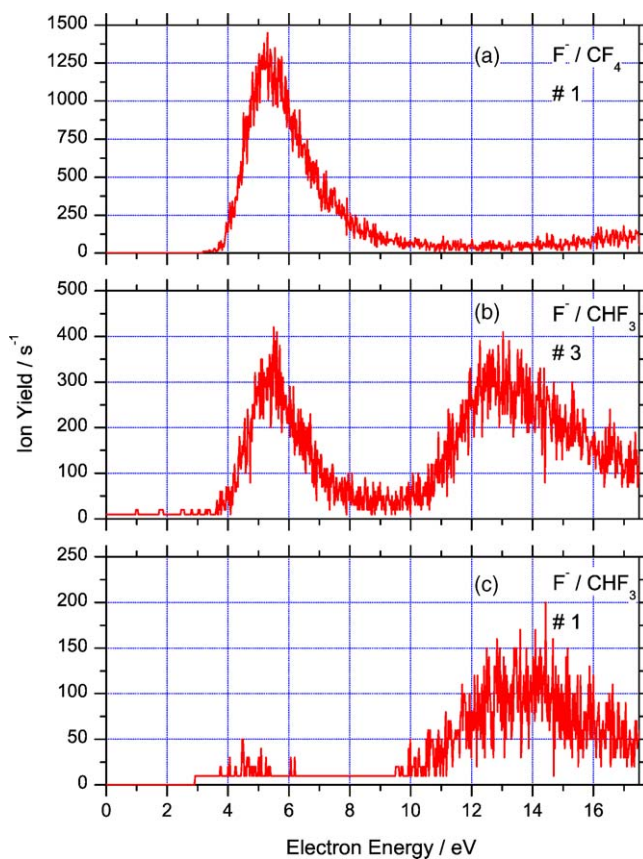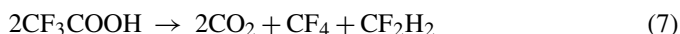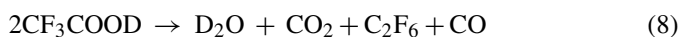

Fig. 4. F^-/ESD yields: (a) first scan from a freshly deposited film of CF_4 (#1), (b) third scan from a freshly deposited film of CHF_3 (#3) and (c) first scan from the same film. The sequence indicates fast transformation of CHF_3 into CF_4 under electron impact in the range 0–17.5 eV.

signal in the range 12–16 eV. After successive scans a new desorption feature peaking at 5.5 eV appears which gradually becomes the dominant contribution, see Fig. 4b. This low energy feature closely resembles the F^-/CF_4 ESD yield obtained from a freshly deposited pure CF_4 film (Fig. 4a). We hence conclude that CHF_3 is rapidly transformed into the thermodynamically more stable compound CF_4. It should be mentioned that both CF_4 and CHF_3 generate a very similar TDS feature (recorded on the CF_3^+ signal representing the dominant peak in the mass spectrum of both compounds). We finally note that a series of more cations are observed in the mass spectrum of the desorbed material (CF^+, CF_2^+, CF_3^+, CF_2H^+) arising from the initial molecule or electron induced products. They show similar desorption features as those discussed above.

For the chemical reactions induced in the CF_3COOH film as observable via ESD and TDS we finally propose the following reactions. At a threshold near 3 eV electron impact leads to homolytic C–C bond cleavage:

$$CF_3COOH \rightarrow CF_3 + COOH \qquad (6)$$

with both radicals desorbing at some lower temperature than the initial molecule. In addition, transformation into CO_2 and CHF_3 (reaction (5)) occurs via secondary reactions induced by electrons. The evolution of the F^-/CHF_3 ESD spectra further

indicates the transformation of CHF_3 into CF_4 (Fig. 4). The resulting overall reaction can then be summarized as

$$2CF_3COOH \rightarrow 2CO_2 + CF_4 + CF_2H_2 \qquad (7)$$

In the gas phase this reaction is exothermic ($-105\,kJ\,mol^{-1}$, Table 1). We will not speculate on the detailed mechanisms and sequences of these reactions but note that they are most likely initiated through electronically excited states of neutral CF_3COOH.

As mentioned above, electron attachment in clusters generates the ion molecule complex $CF_3COO^- \cdot H_2O$ as strongest signal peaking at 0.4 eV via the low energy shape resonance. To obtain information whether such a reaction also takes place in condensed CF_3COOH, we have performed extended irradiation experiments on CF_3COOD. We used the deuterated analogue to distinguish from possible signals due condensation of H_2O which is always present to some extend in the background gas. The observation is that the TDS spectrum in fact gives a signal at 20 amu (D_2O^+), arising within a desorption feature in the same temperature range where CF_3COOD desorbs. This signal, however, is already present by desorbing the non-irradiated film. It should be mentioned that from the thermodynamic point of view, CF_3COOD is an unstable species and the reaction generating water:

$$2CF_3COOD \rightarrow D_2O + CO_2 + C_2F_6 + CO \qquad (8)$$

is slightly exothermic ($-27\,\text{kJ}\,\text{mol}^{-1}$), but in the gas phase kinetically hindered by large activation barriers. One can hence not exclude that the metal surface acts as a catalyst for reaction (8). Desorption of the non-irradiated film, however, does not give evidence for the presence of CO_2 and the presence of C_2F_6 would generate an F^- resonance in ESD peaking at 3.9 eV [27]. The absence of this resonance does not point to a catalytic reaction in the non-irradiated film.

On the basis of the material available so far we have no indication that H_2O is generated at low energies. In fact, the cluster experiments showed that this reaction is essentially restricted to the dimer [2] and it is hence likely, that this channel is completely quenched by a larger dissipative environment.

4. Conclusions

In conclusion the present system CF_3COOH apparently shows remarkable effects at any stage of aggregation on the route from single gas phase molecules over clusters to the condensed material. While the gas phase molecules possess a pronounced low energy shape resonance leading to the loss of H and HF, electron attachment to dimers of CF_3COOH triggers water formation observable on the ion-molecule complex $CF_3COO^- \cdot H_2O$ as the most abundant ion of the negative ion mass spectrum recorded at 0.4 eV. Electron impact to condensed CF_3COOH/CF_3COOD finally induces the desorption of H^-/D^- and F^- via resonant features in the range 5–12 eV, similar to the high energy DEA features from gas phase CF_3COOH. In addition, extended irradiation of the film generates CO_2 and CHF_3/CF_4 as observed via ESD and TDS.

References

[1] J. Langer, M. Stano, S. Gohlke, V. Foltin, S. Matejcik, E. Illenberger, Chem. Phys. Lett. 419 (2005) 228.

[2] J. Langer, I. Martin, G. Karwasz, E. Illenberger, Int. J. Mass Spectrom. Ion Processes 249/250 (2006) 477.

[3] B.L. Nilsson, M.B. Soellner, R.T. Raines, Ann. Rev. Biophys. Biomol. Struct. 34 (2005) 91.

[4] R. Arnold, W. Azzam, A. Terfort, C. Wöll, Langmuir 18 (2003) 3980.

[5] S.R. Müller, H. Frank, Umwelt 2 (1999) (Bundesamt für Umwelt, Wald und Landschaft, Bern, Schweiz).

[6] T. Sommerfeld, H.-D. Meyer Meier, L.S. Cederbaum, Phys. Chem. Chem. Phys. 42 (2004) 42.

[7] L. Sanche, J. Phys. B: At. Mol. Opt. Phys. 23 (1990) 1597.

[8] R. Balog, J. Langer, S. Gohlke, M. Stano, H. Abdoul-Carime, E. Illenberger, Int. J. Mass Spectrom. 233 (2004) 267.

[9] R. Balog, N. Hedhili, F. Bournel, M. Penno, M. Tronc, R. Azria, E. Illenberger, Phys. Chem. Chem. Phys. (PCCP) 4 (2002) 3350.

[10] T. Sedlacko, R. Balog, A. Lafosse, M. Stano, S. Matejcik, R. Azria, E. Illenberger, Phys. Chem. Chem. Phys. (PCCP) 7 (2005) 1277.

[11] A. Stamatovic, G.J. Schulz, Rev. Sci. Instrum. 41 (1970) 423.

[12] M. Tronc, R. Azria, Y. Le Coat, E. Illenberger, J. Phys. Chem. 100 (1996) 14745.

[13] R. Balog, E. Illenberger, Phys. Rev. Lett. 91 (2003) 213201.

[14] F.A. Gianturco, R.R. Luchese, J. Langer, I. Martin, M. Stano, G. Karwasz, E. Illenberger, Eur. Phys. J. D 35 (2005) 399.

[15] A. Pelc, W. Sailer, P. Scheier, M. Probst, N.J. Mason, E. Illenberger, T.D. Märk, Chem. Phys. Lett. 361 (2002) 277.

[16] W. Sailer, A. Pelc, M. Probst, J. Limtrakul, P. Scheier, E. Illenberger, T.D. Märk, Chem. Phys. Lett. 378 (2003) 250.

[17] V.S. Prabhudesai, A.H. Kelkar, D. Nandi, E. Krishnakumar, Phys. Rev. Lett. 95 (2005) 143202.

[18] M. Meinke, E. Illenberger, J. Phys. Chem. 98 (1994) 6601.

[19] W.-F. Schmidt, Liquid State Electronics of Insulating Liquids, CRC Press, Boca Raton, 1997.

[20] E. Illenberger, J. Momigny, Gaseous Molecular Ions, Steinkopff Darmstadt, Springer, New York, 1992.

[21] H.Y. Afeefy, J.F. Liebman, S.E. Stein, in: P.J. Linstrom, W.G. Mallard (Eds.), NIST Chemistry WebBook, NIST Standard Reference Database Number 69, National Institute of Standards and Technology, Gaithersburg, MD, 2005 (http://webbook.nist.gov); S.G. Lias, J.E. Bartmess, J.F. Liebman, J.L. Holmes, R.D. Levin, W.G. Mallard, in: P.J. Linstrom, W.G. Mallard (Eds.), NIST Chemistry WebBook, NIST Standard Reference Database Number 69, National Institute of Standards and Technology, Gaithersburg MD, 2005 (http://webbook.nist.gov).

[22] S. Lacombe, F. Cemic, K. Jacobi, M.N. Hedhili, Y. Le Coat, R. Azria, M. Tronc, Phys. Rev. Lett. 79 (1997) 1146.

[23] M. Lepage, M. Michaud, L. Sanche, J. Chem. Phys. 113 (2000) 3602.

[24] NIST Mass Spec Data Center, S.E. Stein (Director), in: P.J. Linstrom, W.G. Mallard (Eds.), NIST Chemistry WebBook, NIST Standard Reference Database Number 69, National Institute of Standards and Technology, Gaithersburg MD, 2005 (http://webbook.nist.gov).

[25] CTI Cryogenics, Technical Report.

[26] M. Bertin, I. Martin, A. Lafosse, E. Illenberger, R. Azria, in preparation.

[27] F. Weik, E. Illenberger, J. Chem. Phys. 103 (1995) 1406.